Nonlinear Phenomena in Complex Systems, vol. 18, no. 2 (2015), pp. 259 - 265

Effect of Weak Dissipation on The Dynamics of Multidimensional Hamiltonian Systems

E. V. Felk and A. V. Savin*
Saratov State University, Saratov, RUSSIA

A. P. Kuznetsov†
Saratov Branch of the Institute of Radio-Engineering and Electronics of RAS, Saratov, RUSSIA
(Received 1 April, 2015)

We discuss the effect of weak dissipation on the system with Arnold diffusion which consists of two coupled twist maps. The finite time Lyapunov exponents are used to analyze the dynamics. We observe the phenomenon of transient chaos and changes in the phase space structure including the disappearance of some resonances.

PACS numbers: 05.45.Pq,05.40.Fb
Keywords: Arnold diffusion, weakly dissipative systems, transient chaos, conservative systems

1. Introduction

It is well known that dissipative and conservative systems demonstrate dramatically different types of dynamics. In particular, chaos in non-integrable conservative systems can be observed for almost any parameters, but typically in a very narrow region of the phase space. Otherwise, in dissipative systems chaos appears only in the specific range of parameters but the basin of the chaotic regime usually is rather large [1-4]. If one introduces a small dissipative perturbation into a conservative system it goes into a specific "borderline" state, where both features of conservative and dissipative dynamics should be observed in some way. The peculiarities of systems with weak dissipation including the coexistence of large number of regular attractors and scenarios of transition to chaos were studied in several recent works [5-16]. However, those works mainly concern with the systems with two degrees of freedom. At the same time the structure of phase space of the systems with more then two degrees of freedom differs significant because the resonance layers intersect each other, forming a dense web. It makes the diffusion possible for arbitrary small values of perturbation (Arnold diffusion)[17].
The present work studies the effect of weak fixed dissipation on the dynamics of a system with Arnold diffusion.

2. Two coupled twist maps

Let us consider the system of two coupled twist maps [18-20]:

$$\begin{cases} \varphi_{1_{n+1}} = \varphi_{1_n} + I_{1_n}, \\ I_{1_{n+1}} = I_{1_n} + \varepsilon \frac{\partial f}{\partial \varphi_1}(\varphi_{1_n} + I_{1_n}, \varphi_{2_n} + I_{2_n}), \\ \varphi_{2_{n+1}} = \varphi_{2_n} + I_{2_n}, \\ I_{2_{n+1}} = I_{2_n} + \varepsilon \frac{\partial f}{\partial \varphi_2}(\varphi_{1_n} + I_{1_n}, \varphi_{2_n} + I_{2_n}). \end{cases} \quad (1)$$

Here $f(\varphi_1, \varphi_2) = \frac{1}{\cos\varphi_1 + \cos\varphi_2 + 4}$. For small ε this system can be interpreted as the Póincare map with the section plane φ_3=const for the system with Hamiltonian $H_\varepsilon = \frac{I_1^2}{2} + \frac{I_2^2}{2} + I_3 + \varepsilon f(\varphi_1, \varphi_2)$ which has three degrees of freedom. So parameter ε can be interpreted both as the coupling amplitude for coupled twist maps and the non-integrable perturbation amplitude for Hamiltonian system. The structure of the actions plane (I_1,I_2) seems to be the most informative because for an integrable system the orbit is

*E-mail: avsavin@rambler.ru
†also at Saratov State University, Saratov, RUSSIA

completely determined by actions, so the actions can be interpreted as parameters as well. Also as for Hamiltonian system the frequency is determined as $\omega = \frac{\partial H}{\partial I}$, own frequencies are equal to actions in the system under investigation, so the resonance conditions for system (1) can be written as $k_1 I_1 + k_2 I_2 + 2\pi k_3 = 0$, where k_1, k_2, k_3 are integer. Fig. 1 shows some of resonance lines.

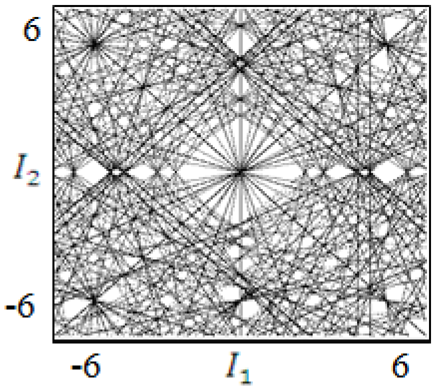

FIG. 1. Resonance lines on the actions plane of the system (1).

To investigate the system (1) we calculate numerically the largest Lyapunov exponent and plot its values on the actions plane (Fig. 2, upper row). The resonance (Arnold) web formed by the regions of chaotic regimes with largest values of Lyapunov exponent is clearly seen. Also we can see that the web structure becomes non-sharp and Lyapunov exponent increases on the average with the increase of coupling amplitude ε, which indicates the growth of diffusion's rate and is rather natural as ε is non-integrable perturbation. On the "action-angle" plane there is a typical set of stochastic layers corresponding to the different orders of resonances and KAM tori with the diffusion over them due to high dimension of the system (Fig. 2, lower row).

3. The effect of linear dissipation

Let us introduce linear dissipation into initial system (1) as follows:

$$\begin{cases} \varphi_{1_{n+1}} = \varphi_{1_n} + I_{1_n}, \\ I_{1_{n+1}} = \alpha I_{1_n} + \varepsilon \frac{\partial f}{\partial \varphi_1}(\varphi_{1_n} + I_{1_n}, \varphi_{2_n} + I_{2_n}), \\ \varphi_{2_{n+1}} = \varphi_{2_n} + I_{2_n}, \\ I_{2_{n+1}} = \alpha I_{2_n} + \varepsilon \frac{\partial f}{\partial \varphi_2}(\varphi_{1_n} + I_{1_n}, \varphi_{2_n} + I_{2_n}). \end{cases} \tag{2}$$

The Jacobian of the system (2) is equal to α so the system is conservative for α=1 and dissipative if α<1. We obtain that regular attractors (mainly fixed points and cycles) occur in the system (2) when one introduces dissipation. Although the number of coexisting attractors can be rather large, the basin of fixed point in the origin occupies the main part of phase space, and only few of other attractors have appreciable basins (see Fig. 3).

3.1. Chaotic transient process

In spite of attractors appearance, the structure of actions plane is similar to that for conservative case if we use finite time Lyapunov exponent with not very long (approx. 1000 iterations) realization length (Fig. 4b). In particular, the resonance web is clearly seen here although it is not so sharp as on Fig. 2. This structure disappears when the realization used for calculation Lyapunov exponent becomes longer (see Fig. 4a, 10000 iterations used). So we can suppose that chaotic transient process takes place in the system. Fig. 4c shows the dependence of transition process duration (i.e. the number of iterations required for initial point to came closer then 10^{-6} to attractor) on the initial conditions (the darker color means the greater number of iterations.) We can see that the transition process is the longest if point starts from initial conditions taken from the resonance region.

Fig. 5 shows the dependence of finite time Lyapunov exponent over the realization length

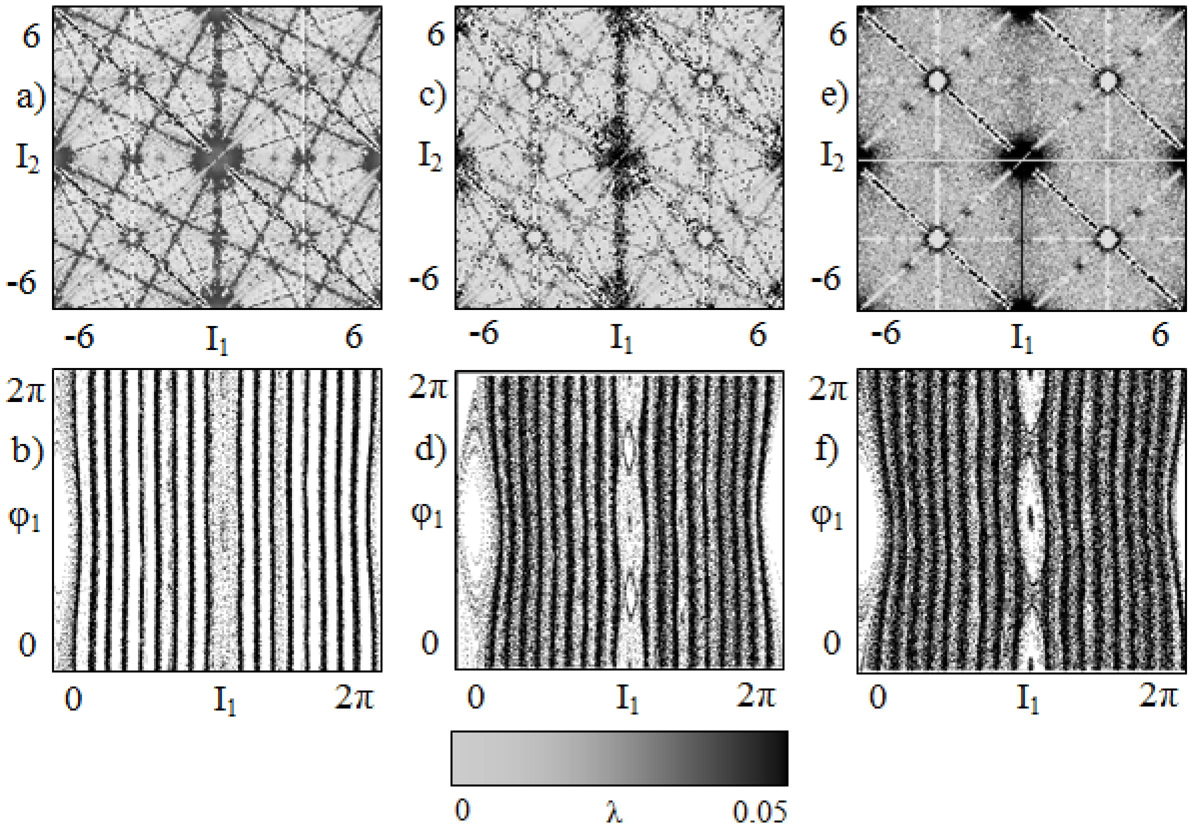

FIG. 2. The values of largest Lyapunov exponent of the system (1) plotted on the actions plane (upper row) and phase portraits in the plane of the "action-angle"(bottom row) at different values ε: a–b) ε=0.3; c–d) ε=0.6; e–f) ε=0.8. More dark color is for larger Lyapunov exponent value.

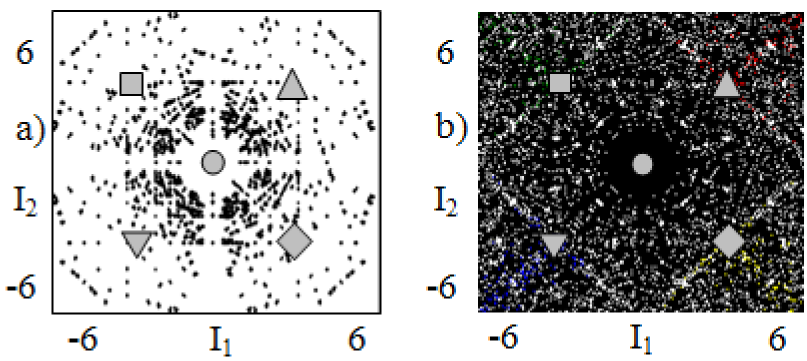

FIG. 3. Attractors (a) and their basins (b) for the system (2) with $\alpha = 0.9999$, ε=0.6. The attractors with largest basins are marked with squares and triangles. Black color on fragment b means the basin of central attractor.

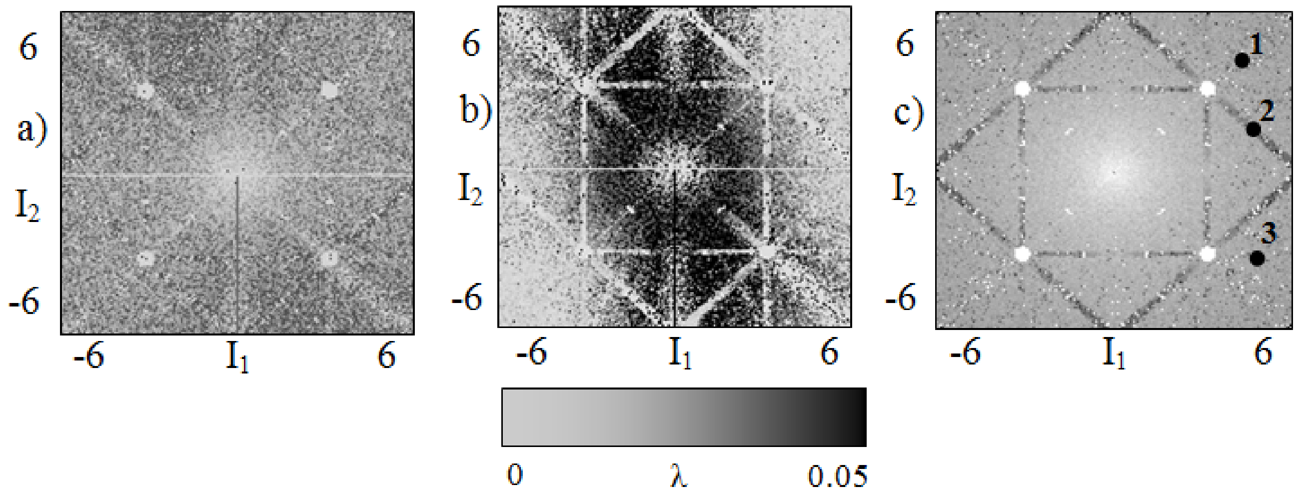

FIG. 4. Maps for the system (2) with $\alpha = 0.999$, ε=0.6. (a–b) maps of Lyapunov exponents and different values N of realization length: $N = 10000$ (a), 1000 (b) iter. (c) Map of transition process duration. Numbered points are the initial conditions used for orbits on Fig. 5.

N for orbits, starting from different points in the plane $(I_1,\ I_2)$, and corresponding phase portraits. We can see that each plot consists of two stages: on the first Lyapunov exponent is definitely positive and changes in a complex way, otherwise during the second stage Lyapunov exponent decreases monotonically to zero. It seems natural to refer the first stage as the chaotic transient process and the second as regular transient process. The plots are qualitatively the same for all initial conditions except the close vicinity of the attractors. On the phase portraits (Fig. 5, right column) the first stage is marked with black points and the second – with gray points. We can see that during the chaotic process the point moves along the resonance lines while during the regular process the point moves near the attracting fixed point. These results show that a set with chaotic behavior exists and is situated along the resonance lines in the action space which results in the chaotic transient process. The length of this process can be approximately determined by the latest spike on the Lyapunov exponent plot and its typical values are near 2000 iterations for the dissipation level $\alpha = 0.999$. The dependence of chaotic transient process length on the initial conditions is shown on Fig. 6. This figure is similar to Fig. 4c which means that the chaotic transient process contributes significantly to the whole transient process.

3.2. The degradation of resonances

Now let us study how the structure of the chaotic set depends on the dissipation level α. We plot the dependence of the finite time Lyapunov exponents with realization length equal to the chaotic transient time on initial conditions (Fig. 7, upper row). For nearly conservative case ($\alpha = 0.999$), the resonant lines are clearly seen although the structure is more diffuse then for the conservative case (Fig. 2c) and the value of the Lyapunov exponent increases in the center of the plane.

It should be marked that some of the regions of chaotic dynamics situated along the resonance lines disappear with the increase of dissipation. For example, a diagonal lines, clearly seen for $\alpha = 0.9$, totally disappear at $\alpha = 0.5$ (Fig. 7c, e), and the resonant web becomes square lattice-like. Also black areas, which correspond to negative values of the finite time Lyapunov exponent (i.e., regular

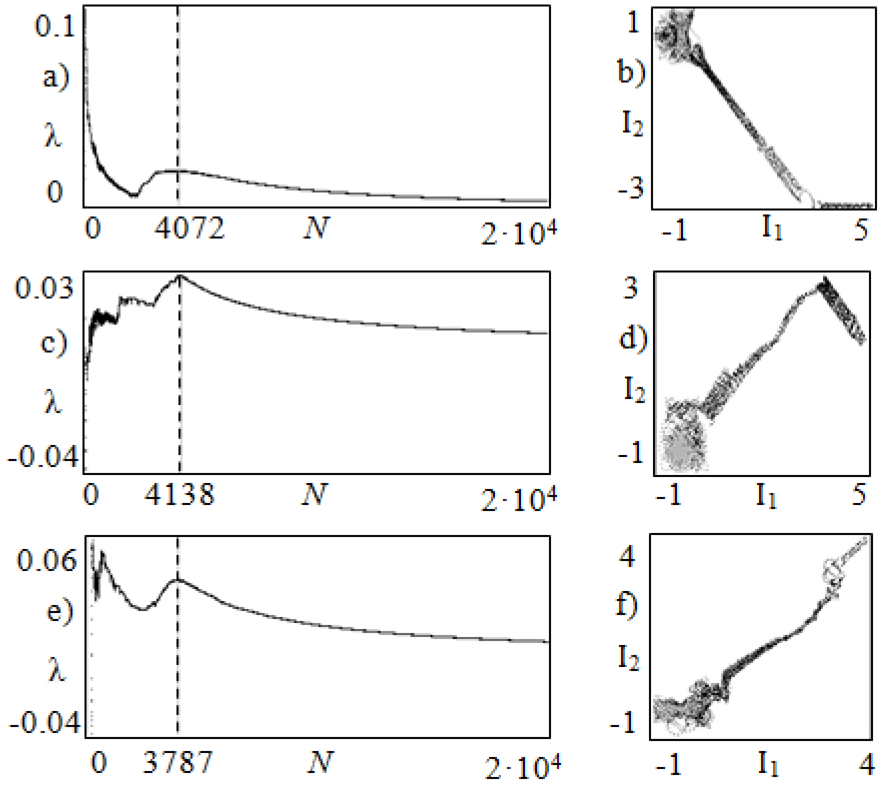

FIG. 5. Dependence of finite time Lyapunov exponent on the realization length N for points marked on Fig. 4c: point 1 – a, b; point 2 – c, d; point 3 – e, f, and corresponding phase porters for the system (2) with $\alpha = 0.999$, $\varepsilon = 0.6$

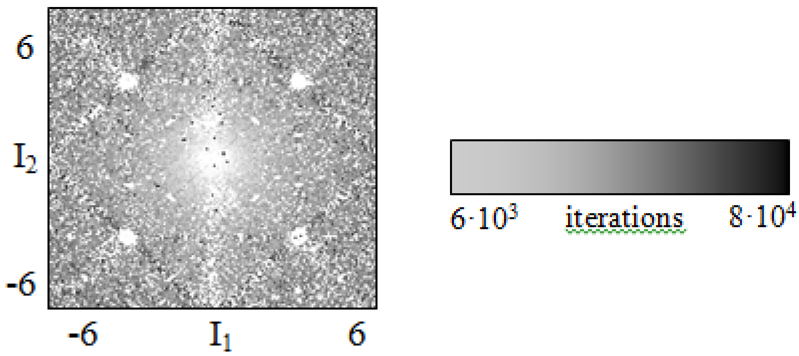

FIG. 6: Map of the duration of the chaotic transition process for the system (2) for $\alpha = 0.999$, $\varepsilon = 0.6$.

dynamics) , appear on the actions plane (Fig. 7e). For larger dissipation values the number of cells is reduced and the areas with regular dynamics become larger.

4. Conclusion

It was found that although regular attractors occur for even small values of dissipation ($\alpha = 0.999$) the sets with chaotic behavior along the

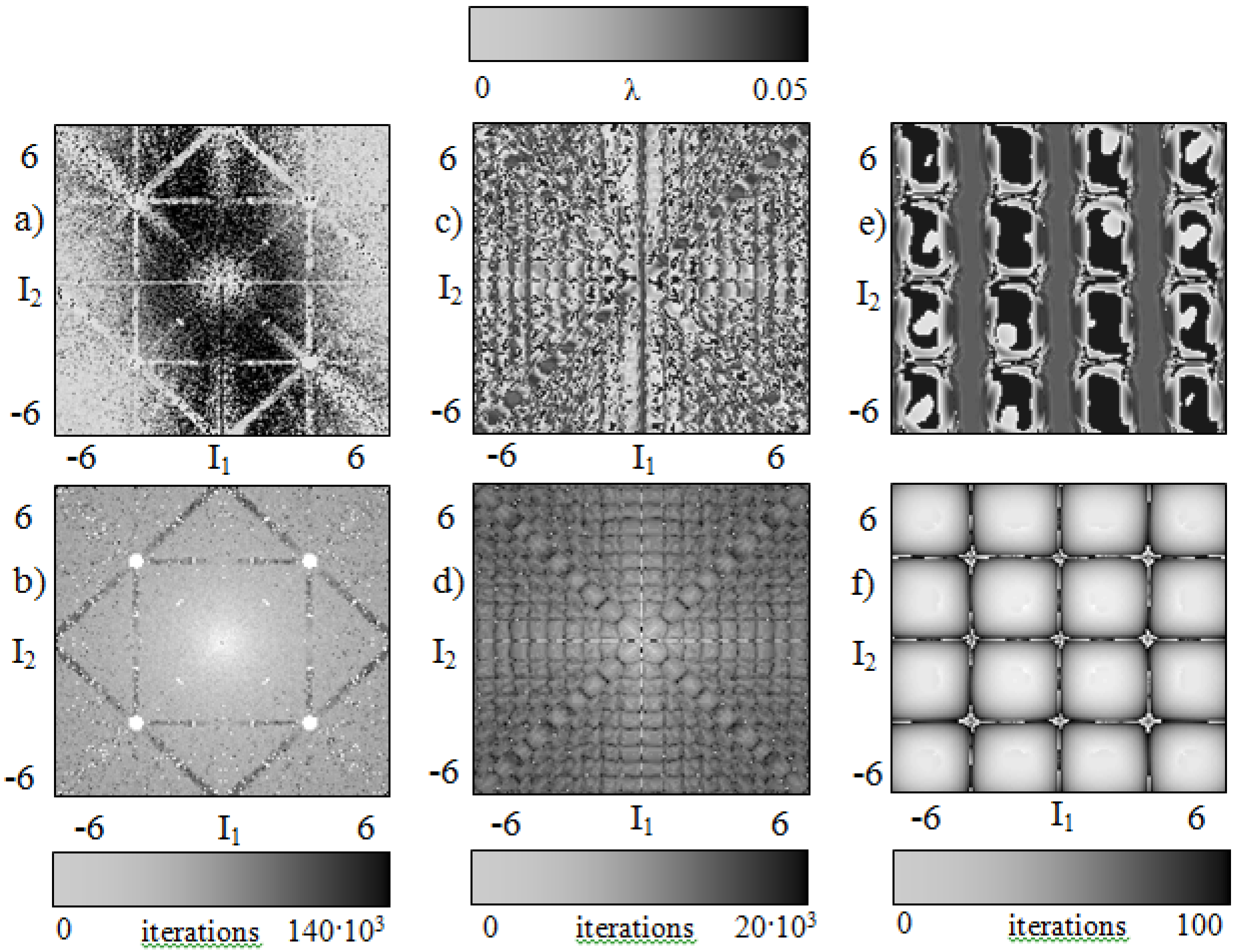

FIG. 7. Maps of dynamical regimes (upper row) and maps the duration of the transition process (lower row) for the system (2) with $\varepsilon = 0.6$ and different values α: 0.999 (a–b); 0.9 (c–d); 0.5 (e–f). Color palettes for Lyapunov exponent λ is in the top, color palettes for transient processes length are in the bottom.

resonance web still exist which results in chaotic transition process. The structure of this set changes with the increase of dissipation resulting in the square lattice without diagonal directions.

Acknowledgments

The authors thank Ph.D. D. V. Savin for useful discussions and Russian Foundation for Basic Researches (projects 15-02-02893 and 14-02-31067) for financial support. E.F. also thanks Dynasty Foundation for financial support.

References

[1] G.M. Zaslavsky, R.Z. Sagdeev, D.A. Usikov, A.A. Chernikov. *Weak Chaos and Quasi-Regular Patterns.* (Cambridge University Press, Cambridge, 1991).

[2] G.M. Zaslavsky. *Physics of Chaos in Hamiltonian Dynamics.* (Imperial College Press, London, 1998).

[3] M. Tabor. *Chaos and Integrability in Nonlinear Dynamics.* (Wiley, New York, 1989).

[4] L.E. Reichl. *The Transition to Chaos in Conservative Classical Systems: Quantum Manifestations.* (Springer–Verlag, Berlin, 1992).

[5] U. Feudel, C. Grebogi, B.R. Hunt, J.A. Yorke. Map with more than 100 coexisting low-period periodic attractors. Physical Review. E **54**, no. 1, 71-81 (1996).

[6] A.Yu. Kolesov, N.Kh. Rosov. The nature of the bufferness phenomenon in weakly dissipative systems. Theoretical and Mathematical Physics. **146**, no. 3, 376-392 (2006).

[7] Martins L.C., Gallas J.A.C. Multistability, phase diagrams and statistical properties of the kicked rotor: a map with many coexisting attractors. Int. J. of Bifurcation and Chaos. **18**, no. 6, 1705-1717 (2008).

[8] U. Feudel. Complex dynamics in multistable systems. Int. J. of Bifurcation and Chaos. **18**, no. 6, 1607-1626 (2008).

[9] B. Blazejczyk-Okolewska, T. Kapitaniak. Coexisting attractors of impact oscillator. Chaos, Solitons & Fractals. **9**, 1439-1443 (1998).

[10] Feudel U., Grebogi C. Multistability and the control of complexity. //Chaos, 1997, 7, № 4, pp. 597-604.

[11] U. Feudel, C. Grebogi. Why are chaotic attractors rare in multistable systems? Phys. Rev. Lett. **91**, no. 13, 134102 (2003).

[12] P. Rech, M. Beims, J. Gallas. Basin size evolution between dissipative and conservative limits. Phys. Rev. E **71**, no. 1, 017202 (2005).

[13] A.P. Kuznetsov, A.V. Savin , D.V. Savin. On some properties of nearly conservative dynamics of Ikeda map and its relation with the conservative case. Physica A. **387**, no. 7, 1464-1474 (2008).

[14] V. Sheeja, M. Sabir. Effect of dissipation on the hamiltonian chaos in coupled oscillator systems. Int. J. Bifurcation Chaos. **12**, 859 (2002).

[15] U.A. de Oliveira, E.D. Leonel. The effect of weak dissipation in two-dimensional mapping. Int. J. Bifurcation Chaos. **22**, 1250248 (2012).

[16] A.L. Mondragon, P.H. Richter. Weak dissipation in a hamiltonian map. Int. J. Bifurcation Chaos. **04**, 921 (1994)

[17] V.I. Arnol'd. Instability of dynamical systems with several degrees of freedom. Sov. Math., Dokl. **5**, 581-585 (1964); translation from Dokl. Akad. Nauk SSSR. **156**, 9-12 (1964).

[18] K. Froeschle , E. Lega. Celestial, M.Guzzo. Analysis of the chaotic behavior of orbits diffusing along the Arnold web. Celestial Mechanics and Dynamical Astronomy. **95**, 141-153 (2006).

[19] M. Guzzo, E. Lega, K. Froeschle. First numerical evidence of global Arnold diffusion in quasi-integrable systems. ArXiv:nlin/0407059 [nlin.CD]

[20] M. Guzzo, E. Lega, C. Froeschle. Diffusion and stability in perturbed non convex integrable systems. Nonlinearity. **19**, no. 5, 1049-1067 (2006).